INTERNATIONAL ATOMIC ENERGY AGENCY
UNITED NATIONS EDUCATIONAL, SCIENTIFIC AND CULTURAL ORGANIZATION
INTERNATIONAL CENTRE FOR THEORETICAL PHYSICS
I.C.T.P., P.O. BOX 586, 34100 TRIESTE, ITALY, CABLE CENTRATOM TRIESTE

SMR.762 - 25

SUMMER SCHOOL IN HIGH ENERGY PHYSICS AND COSMOLOGY

13 June - 29 July 1994

PERSPECTIVES IN NUCLEAR PHYSICS

S. FANTONI
SISSA
Trieste

Please note: These are preliminary notes intended for internal distribution only.

Perspectives in Nuclear Physics

S. Fantoni
(SISSA)

1. Introduction
2. The Nuclear Many-Body problem
3. inclusive scattering of GeV electrons
4. diffractive electroproduction of $s\bar{s}$ mesons
5. Conclusions

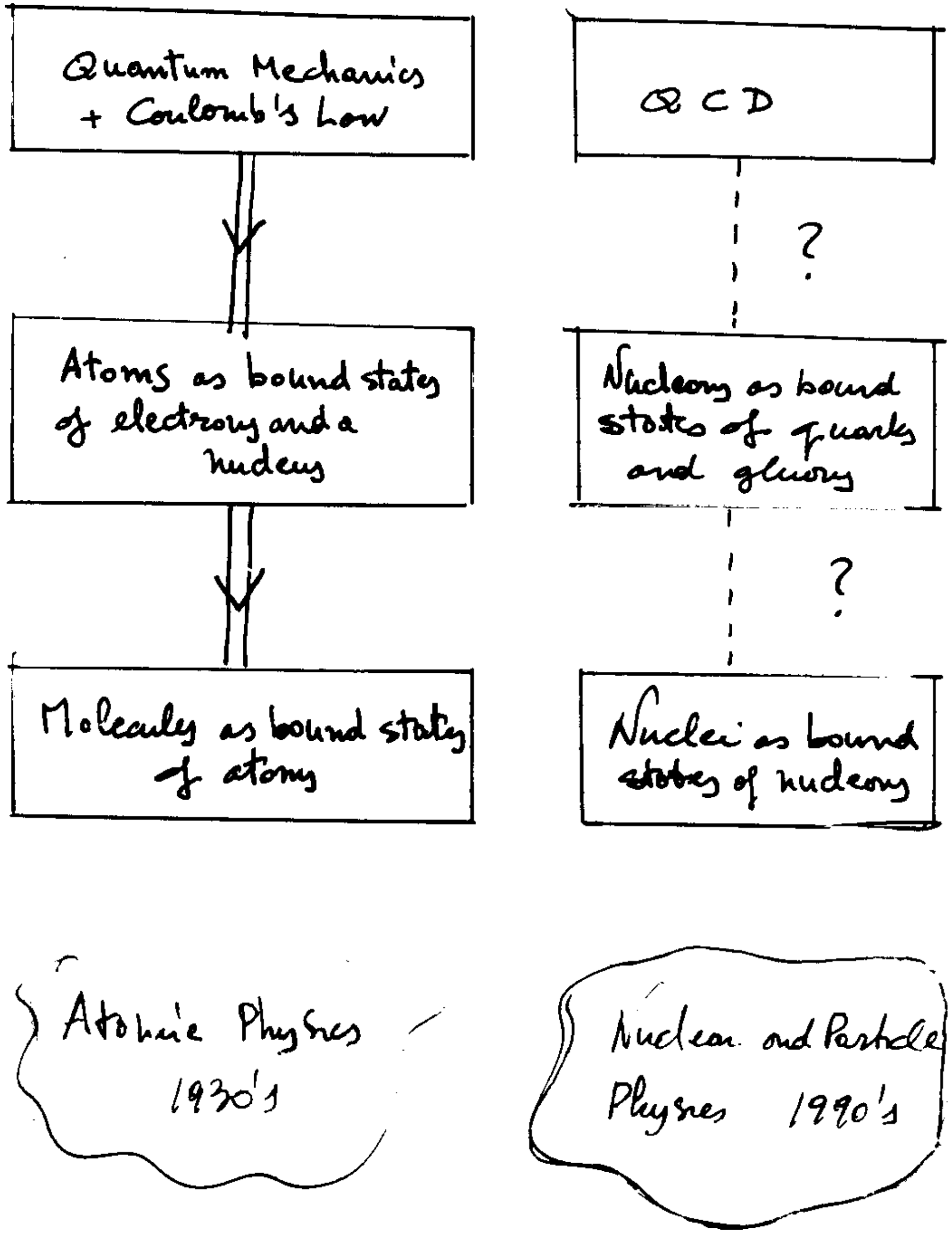

"Atomic Physics"

- quark confinement: flux tubes? bags?
- why qqq & $q\bar{q}$: what is a constituent quark; extra $q\bar{q}$ pairs
- where is the glue: 50% momentum; 0% spectrum

"Molecular Physics"

- why nucleons? versus 3A quarks; exact few body; liquid drops; Repulsive core
- Nature of NN force: meson $\leftrightarrow$ quark exchange; other hadron-hadron forces
- Short distance degrees of freedom: Not NN, but?

flux tubes?
bags?
what is a constituent quark
extra $q\bar{q}$ pairs
50% momentum
0% spectrum
versus 3A quarks
exact few body
liquid drops
Repulsive core
meson $\leftrightarrow$ quark exchange
other hadron-hadron forces
Not NN, but?

— Nuclear Physics (phenomenology)

— QCD

— Condensed matter

— Many-Body

Nucleus as a laboratory for non-perturbative QCD phenomena

↓

propagation of an hadron in nuclear matter

— Fedeev

— FHNC & CBF

— stochastic methods:

- Variational Monte Carlo
- Green Function Monte Carlo
- Path Integral Monte Carlo

"ab initio" calculations

Hadronic matter

— Nuclear matter: Equation of state, Landau parameters, pairing

— Neutron matter: Equation of state + protons + λ's, Superfluidity

— Hot matter: flows etc...

— Phase transitions: quark matter

Condensed Matter Phys.

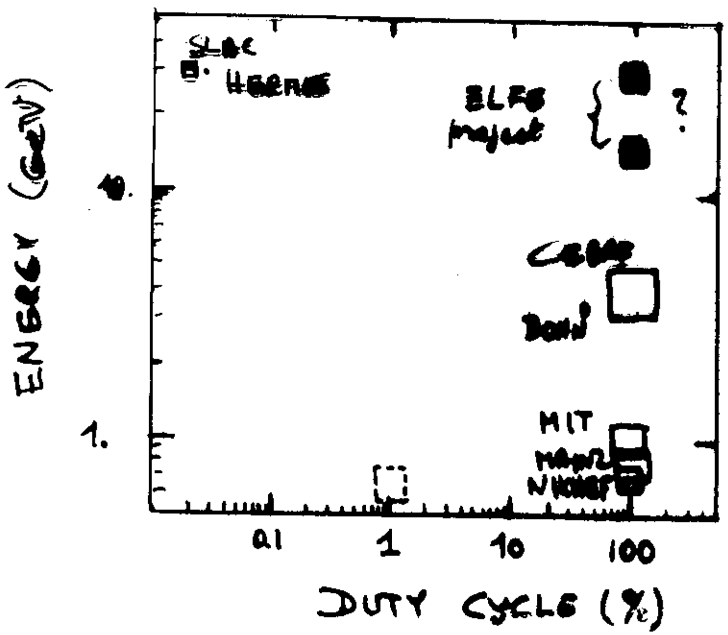

High ENERGY (E ≥ 0.5 GeV) electron facility for HADRONIC STUDIES.
The Area of the square is proportional to the BEAM CURRENT.

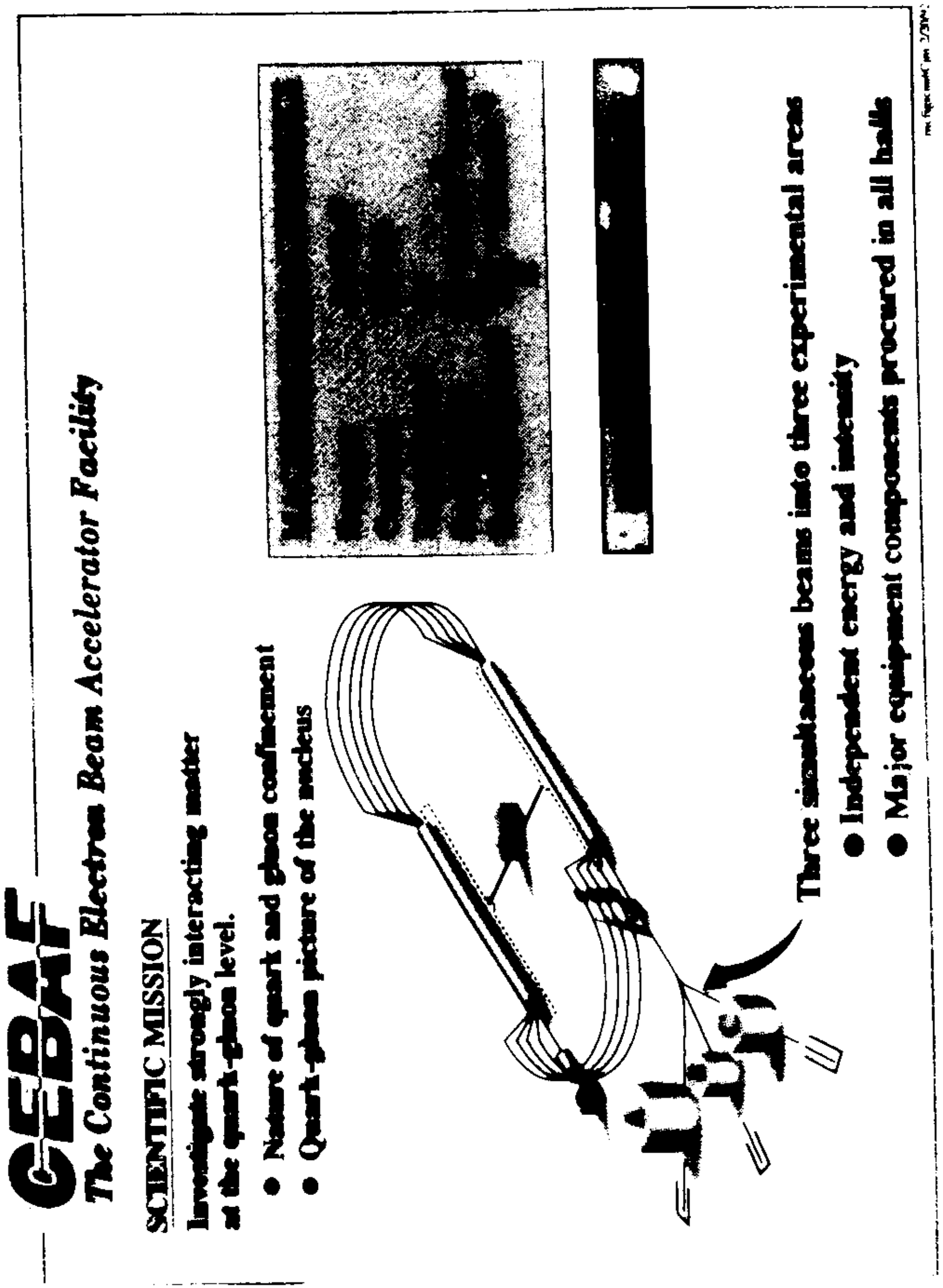

APPEALING FEATURES of CEBAF

- electron scattering is clean - few reaction products

- continuous beam (duty factor 1) & high current (200 microamps)

Burst of electrons separated by NANO seconds
STRING of PEARLS

SLAC (duty factor 10^{-4}) (2 microseconds). The beam is only $\frac{1}{5000}$ of the time
$\Downarrow$
10^4 more electron per "PEARL" < Targets ? / Multiple interactions ?

- small x section & angular divergence (emittance 2.10^{-9} m - radiant)
- small energy spread (10^{-4})
- polarization 50% → 90%
- Tagged photon facility

Nucleon and meson form factors

∴ Charge Form Factor of the neutron (Hall C)

(I. Sick): $\vec{d}(\vec{e}, e') \rightarrow$ Asymmetry measurement
$\Downarrow$
$G_E^n \cdot G_E^m$

∴ (R. Madey): $d(\vec{e}, e'\vec{n})p$

∴ (N.V. Kosnov) Electroproduction of light Quark mesons

$\pi\gamma \rightarrow \pi^*$ transition form factors

(μ, ν, π) DIS

$\rightarrow \langle N | \bar{s}\, \gamma_\mu \gamma_5\, s | N \rangle$

$\langle N | \bar{s}\, \gamma_\mu\, s | N \rangle$

STRANGE QUARKS :

$\boxed{\text{Parity Violation exp. PROGRAM}}$

Measure the s-quark content of the proton $\Rightarrow$ $q\bar{q}$ ocean in the proton

$\Downarrow$

Elastic flavor singlet charge form factor G_E^0

$\Downarrow$

$$A = \frac{\sigma_+ - \sigma_-}{\sigma_+ + \sigma_-} \qquad \text{(elastic e-p)}$$

$\sim 10^{-6}$ less than 5% statistical & systematic accuracy.

quark current $J_\mu^{em} = Q\, \bar{q}\, \gamma_\mu\, q$

coupling appropriate to γ or Z^0

$$G_E^{p,\gamma} = \sum_j Q_j\, G_E^{j,p} = \frac{2}{3} G_E^{u,p} - \frac{1}{3} G_E^{d,p} + \dots$$

$$G_E^{p,Z} = \sum_j \left(\frac{1}{2} T_j^3 - Q_j \sin^2\theta_W\right) G_E^{j,p}$$

$$\rightarrow \left(\frac{1}{2} - \sin^2\theta_W\right) G_E^{p,\gamma} - \frac{1}{4} G_E^{0,p}$$

$$G_E^{0,p} = \frac{1}{3}\left(G_E^{u,p} + G_E^{d,p} + G_E^{s,p}\right)$$

10^{-5} smaller

$$M = M^\gamma + M^Z$$

$$A = \frac{\sigma_+ - \sigma_-}{\sigma_+ + \sigma_-} \propto \frac{M^\gamma M^Z}{|M^\gamma|^2} \qquad \tau = \frac{Q^2}{4M^2}$$

$$= -\frac{G_F Q^2}{\pi\alpha\sqrt{2}} \left[\varepsilon G_E^\gamma G_E^Z + \tau G_M^\gamma G_M^Z - \frac{1}{2}(1 - 4\sin^2\theta_W)(1-\varepsilon^2)^{1/2} \sqrt{\tau(1+\tau)}\, G_M^\gamma G_A^Z\right]$$

$$\times \left[\varepsilon (G_E^\gamma)^2 + \tau (G_M^\gamma)^2\right]^{-1}$$

$\varepsilon = [1 + 2(1+\tau)\operatorname{tg}^2\theta/2]^{-1} \longrightarrow [0, 1]$

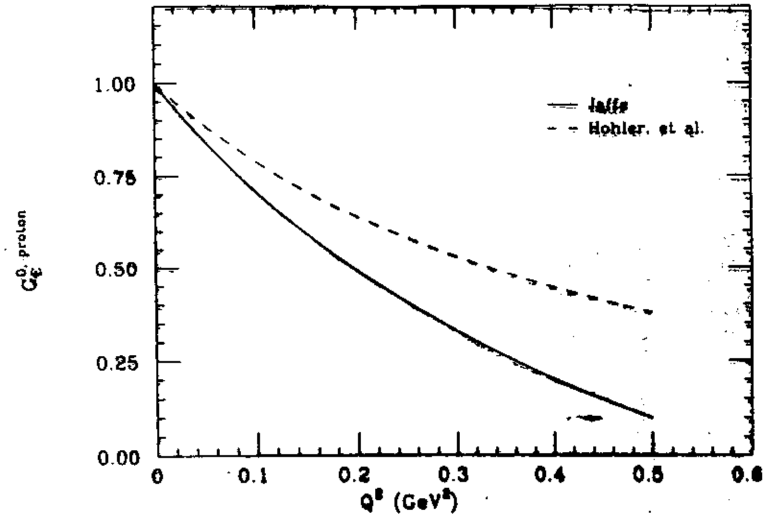

Figure 1: Comparison of G_E^0 as a function of momentum transfer for the form factor fits of Höhler *et al.* [He76] and Jaffe [Ja89]. The Höhler *et al.* fit assumes that there are no strange quarks in the nucleon.

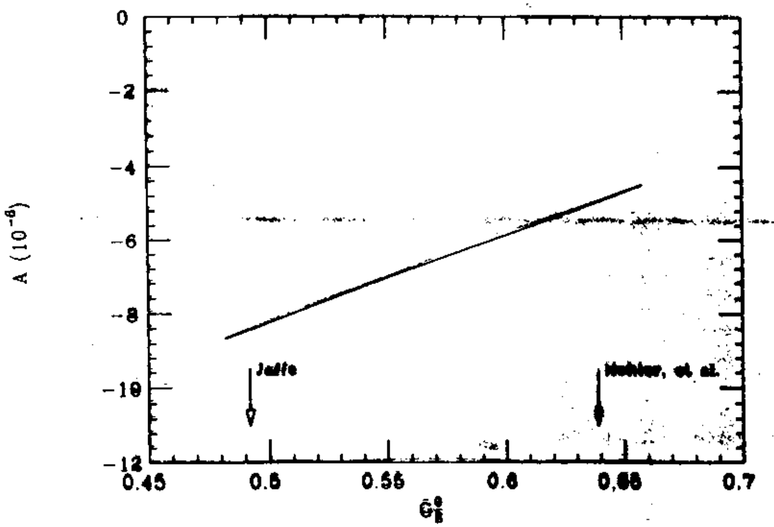

Figure 2: Elastic ep asymmetry at $Q^2 = 0.2$ for the range of G_E^0 values bracketed by the Höhler *et al.* and Jaffe form factors shown in Figure 1.

- Douglas Beck (Urbana)

  e-p at $0.1 \leq Q^2 \leq 0.3\ \mathrm{GeV}^2$

  HALL-C : detect backward protons (dedicated spectrometer)

- E. Beise & R. McKeown (Caltech)

  e-^{4}He ($T=0$, $J=0$ nucleus) at $Q^2 = 0.6\ (\mathrm{GeV}/c)^2$

  $$A = \frac{G_F Q^2}{\pi\alpha\sqrt{2}}\left[\sin^2\theta_W + \frac{1}{2}\frac{G_E^s}{(G_E^p + G_E^n)}\right]$$

  Hall A .

- P. A. Souder (MIT) [SAMPLE]

  e-p & e-^{4}He at $0.27 < Q^2 < 1.3$

  Hall A

HALL A

(42)

~ Approved (e, e'p) experiments (≈ 100 days beam time)

He (e, e'p) J. Mougey

- light nuclei
- reaction mechanism

^{16}O (e, e'p) R. Lourie

- $R_L + \frac{v_{TT}}{v_L} R_{TT}$, R_T, R_{LT} separation

- high missing energy, $E_m \sim 300$ MeV

^{208}Pb (e, e'p) C.N. Papanicolas (CA)

- high momentum component in heavy nuclei
- s.p. strength

A (e, e'$\vec{p}$) A. Saha

D (e, e'$\vec{p}$) J. M. Finn

^{16}O (e, e'$\vec{p}$) C. Glashausser

reaction mechanism
final state interaction
- [illegible]

THEORY

- Theory Centre - SEATTLE

- ECT* - TRENTO

MOTTELSON, BRINK
BLAIZOT, PETHICK, Mueller
WEISE, SPECHT, S.F.

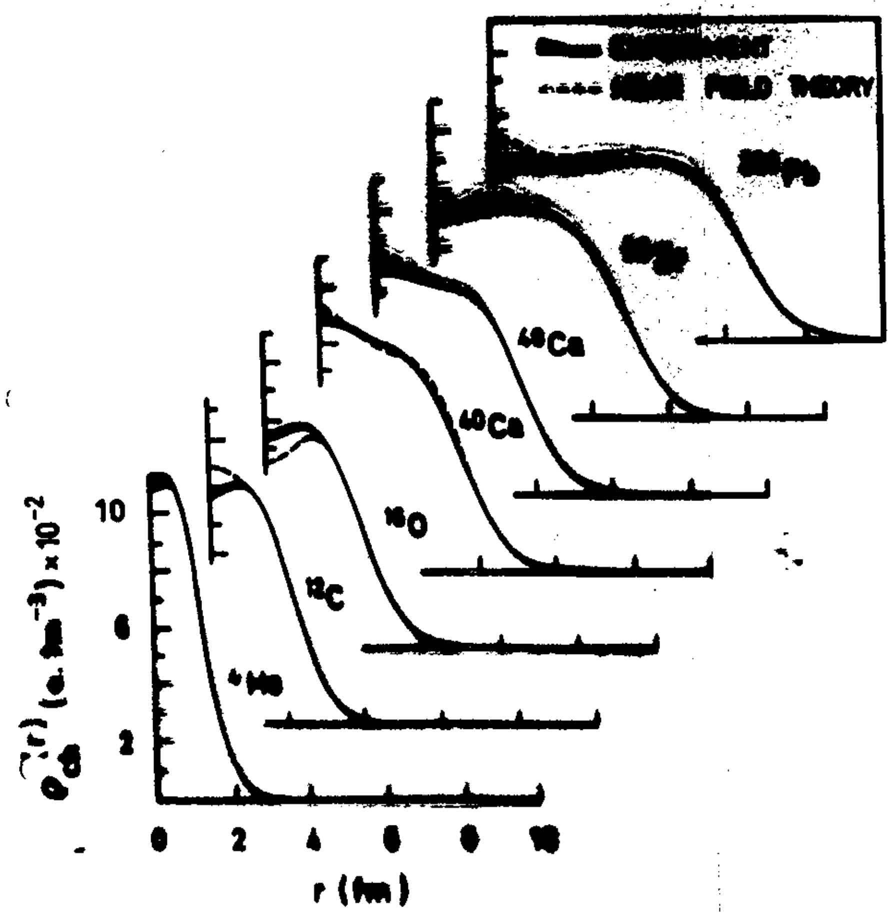
EXPERIMENT
MEAN FIELD THEORY
^{208}Pb
^{40}Ca
^{16}O
^{12}C
^{4}He
10
6
2
0
2
4
6
8
10
r (fm)

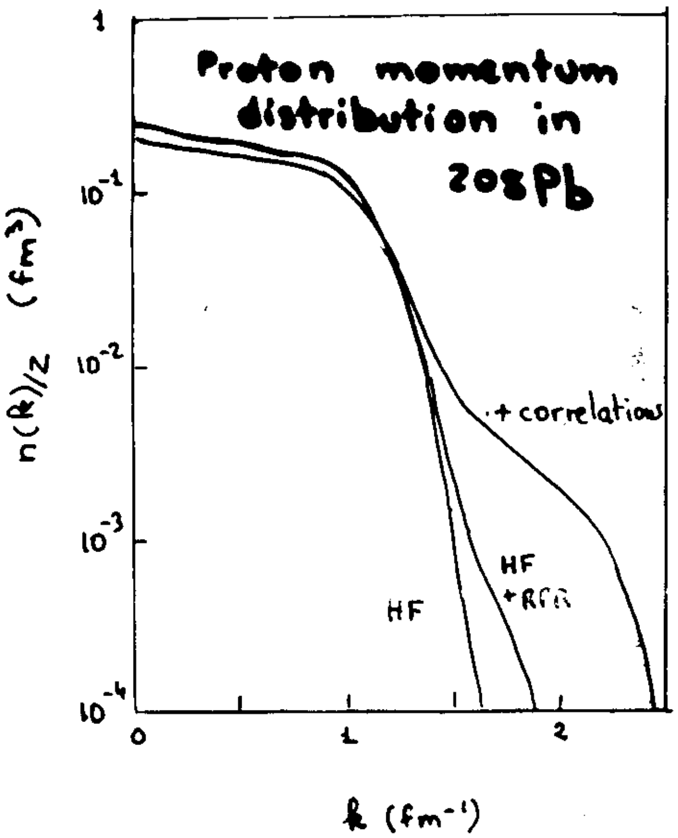
Proton momentum distribution in 208Pb
1
10^{-1}
10^{-2}
10^{-3}
10^{-4}
n(k)/Z (fm^3)
+ correlations
HF
HF + RPA
0
1
2
k (fm^{-1})

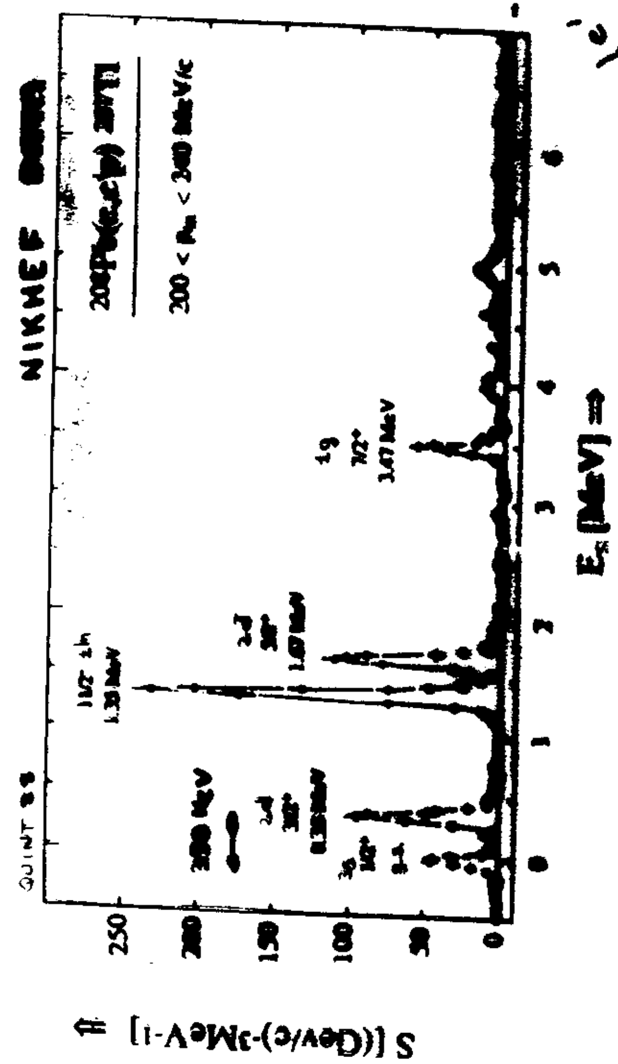

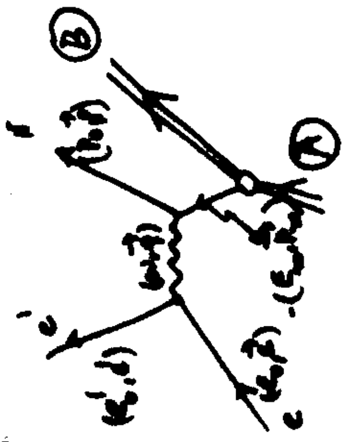

$E_x = E_{sep} - E_m$

Benhar et al

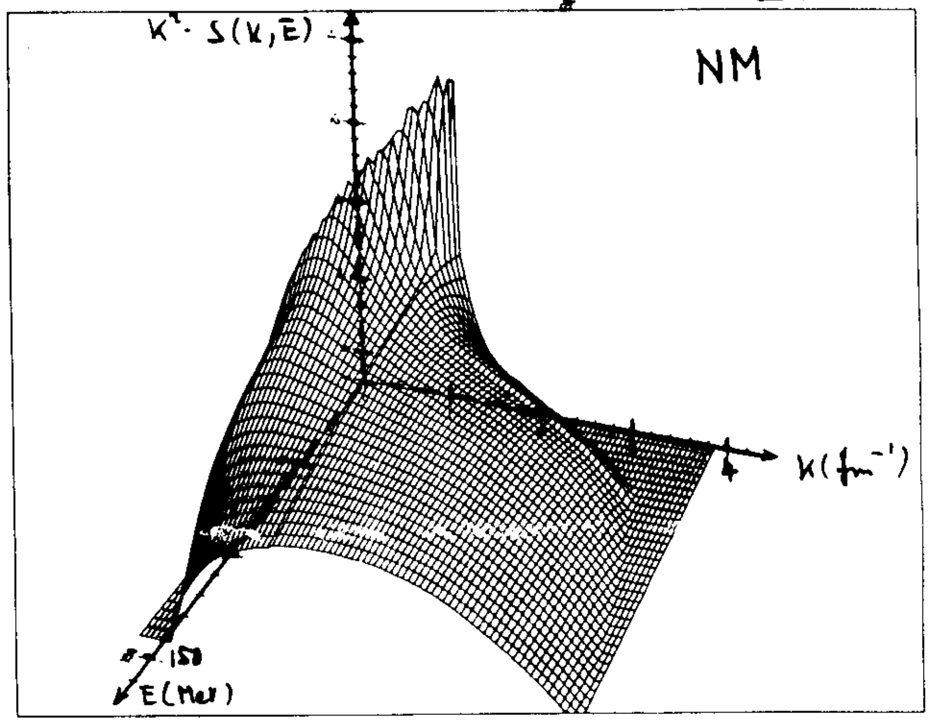

Spectral function of Nuclear Matter

[O. Benhar, A. Fabrocini, S.F. (1989)]

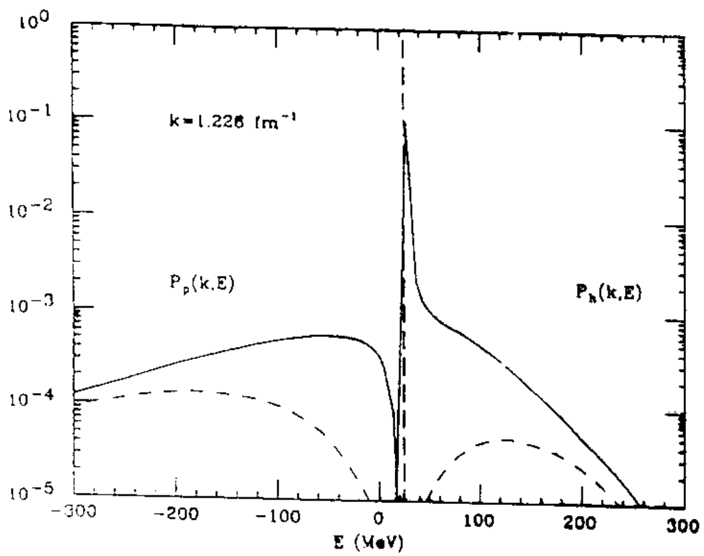

$$P(k,E) = \sum_{\bar{N}} |\langle 0 | a_k^\dagger | \bar{N} \rangle|^2 \delta(E - E_N - E_0)$$

High momentum components in ψ_0

$\langle a_k^\dagger a_k \rangle$

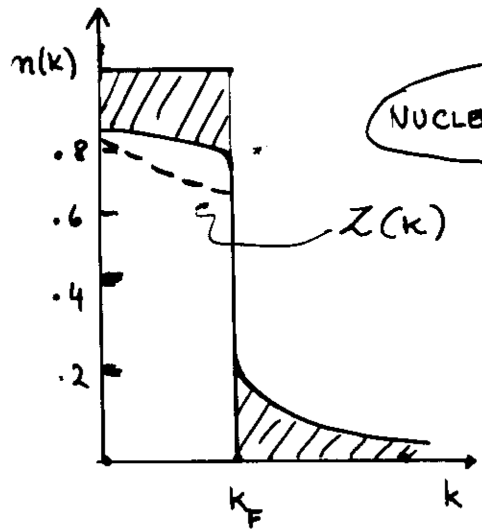

- quenching of s.p. occupation probab. (NIKHEF experiments)
- proton momentum distribution
- charge distribution
- inclusive response

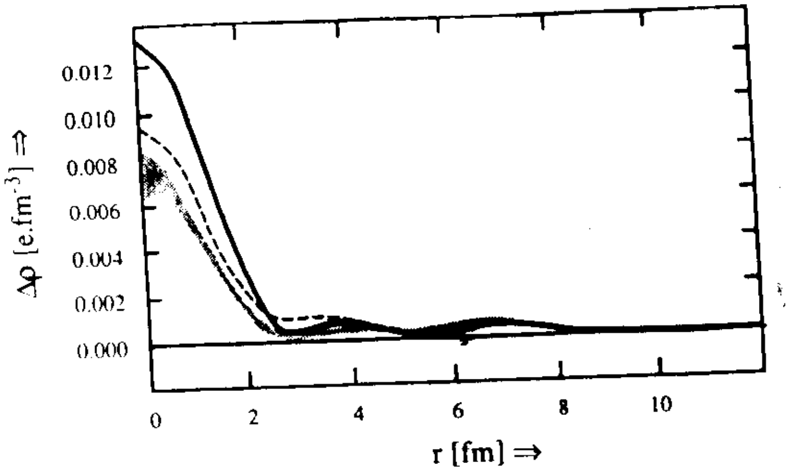

Figure 1.1 Experimental charge-density difference between ^{206}Pb and ^{205}... displaying a clear $3s_{1/2}$ character. The solid curve is the result of a mean fi... calculation, assuming a difference of one $3s_{1/2}$ proton between the two isotones a... the dashed curve is calculated assuming that the difference is due to 0.7 $3s_{1/2}$ a... 0.3 2d proton.

A striking example for the existence of single-particle properties in heavy nu... experimentally determined charge-density difference between the isotones ^{206}Pb ... [CavF-82, FroC-83]. This one-proton difference clearly displays (see figure 1.1) ... character of a $3s_{1/2}$ density, but it is considerably smaller in the center than the density ... for a difference of one $3s_{1/2}$ proton (solid line). It can be described reasonably well wit... difference containing 0.7 $3s_{1/2}$ proton and 0.3 2d proton (dashed line). Therefore ... conclude, that there is an absolute difference of 0.7 proton between the filling of the $3s_{1/2}$ orbit in ^{206}Pb and in ^{205}Tl. It has later also been interpreted as a 70% occupancy of the

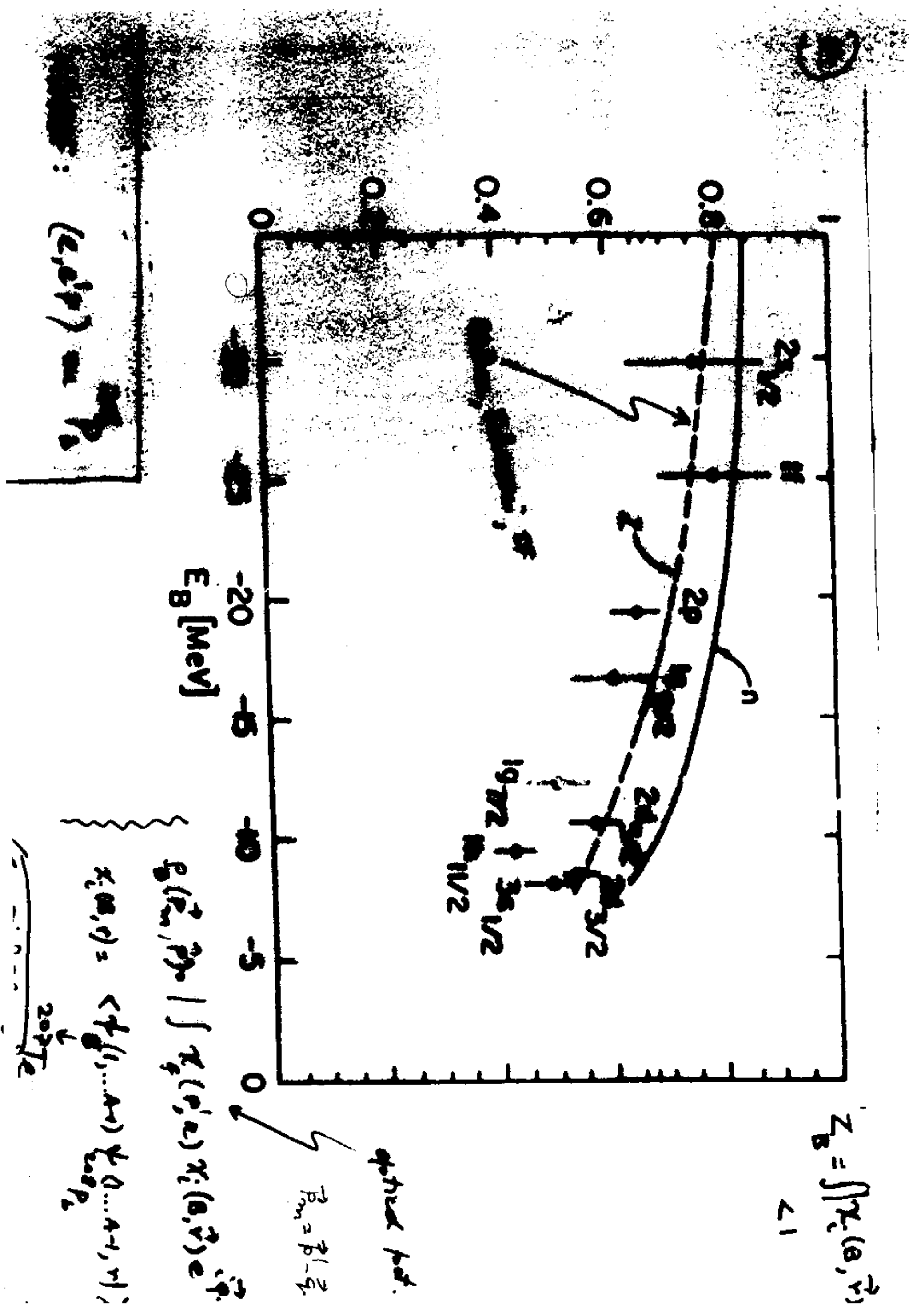

absorption mechanism. Note in the present case (^{16}O) that $E_m \approx 100\ MeV$ for $p_m = 880\ MeV/c$.

That the two-nucleon absorption mechanism is a good hypothesis was established at Saclay for $^3He(e,e'p)$ [9] and $^4He(e,e'p)$ [10] (Fig. 3b, 3b).

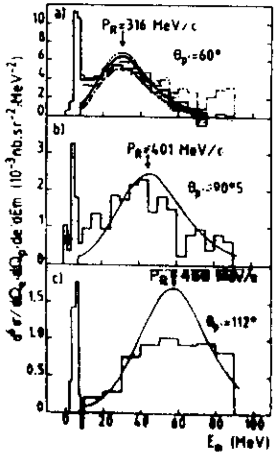

Fig. 3a

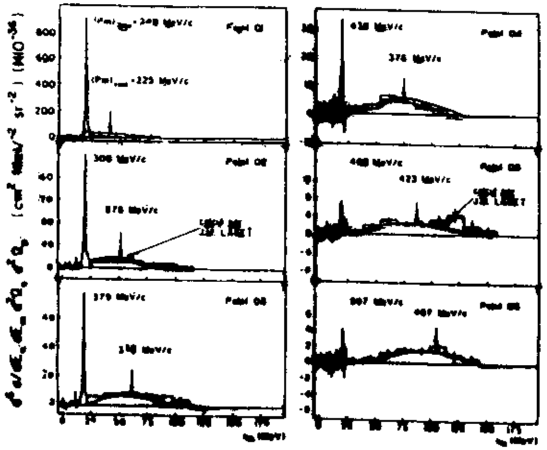

Fig. 3b

As is well known, in plane wave impulse approximation ($PWIA$) (i.e. no FSI, no MEC, ...), we can write for the $(e,e'p)$ cross-section:

$$\frac{d^6\sigma}{d\epsilon' dp' d\Omega_{e'} d\Omega_{p'}} = K\sigma_{ep} S(E_m, p_m), \tag{2}$$

ϵ' is the momentum of scattered electron, p' that of the knocked-out proton and S is the spectral function. The (proton) momentum density distribution $n(k)$ is then simply given by:

$$n(k) = \frac{n(p_m)}{Z} = \frac{1}{Z}\int_0^\infty S(E_m, p_m)\, dE_m, \tag{3}$$

with the normalization:

$$\int n(k) d^3k = 1. \tag{4}$$

Note that in Fig. 1a and 1b the normalitation is sligthly different.

2. Nuclear Many-Body theory

Non-relativistic hamiltonian

$$H = -\frac{\hbar^2}{2m}\sum_{i=1,A}\nabla_i^2 + \sum_{j>i} v_{ij} + \sum V_{ijk} + \ldots\ldots$$

negligible in nuclei (?)

currents

$$J_\mu = \sum_i J_{1,\mu}(i) + \sum_{j>i} J_{2,\mu}(i,j) + \sum J_{3,\mu}(ijk) + \ldots$$

In principle: derive v_{ij}, V_{ijk}, j_1, j_2 .... from a fundamental theory (QCD)

In practice: use N-N scattering data, ^2H, ^3H, ^3He, ^4He and nuclear matter.

Correlations $\Longleftrightarrow$ strongly interacting systems

continuum systems (quantum liquids, helium, NM...)

$$\boxed{H = -\frac{\hbar^2}{2m}\sum_i \nabla_i^2 + \sum_{i<j} v_{ij} + \sum v_{ijk} + \ldots}$$

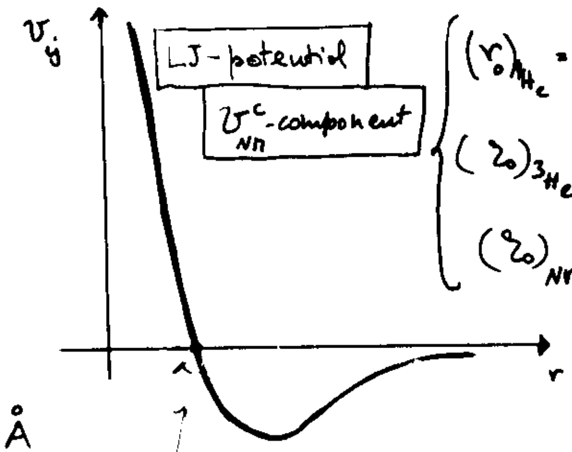

$(r_0)_{{}^4He} = 0.87\,\sigma$

$(r_0)_{{}^3He} = 0.95\,\sigma$

$(r_0)_{NM} = 1.143$ fm

$\sigma = 2.556$ Å

d $\begin{cases} 1.\sigma & \text{for liquid Helium} \\ \sim 1 \text{ fm} & \text{for nuclear matter} \end{cases}$

Lattice systems (s.c. electrons)

$$\boxed{H = -t\sum_{\langle i,j\rangle} c^+_{i\sigma} c_{j\sigma} + U\sum_i n_{i\uparrow} n_{i\downarrow} \qquad n_{i\sigma} = c^+_{i\sigma} c_{i\sigma}}$$

The ground state is approximated by

$$\Phi_0 = \mathcal{A}\prod_i \phi_i(r_i) \Longrightarrow \psi_0 = \hat{G}_{cor}\,\Phi_0$$

weakly interacting $\qquad$ strongly interacting

$$\hat{G}_{cor} = \prod_{i<j} f_2(r_{ij}) \prod_{ijk} f_3(\vec{r}_{ij}, \vec{r}_{ik}) \ldots\ldots$$

$$\times \int \left[\prod_{i<j} F_2(ij) \prod F_3(ijk) \ldots\right]$$

- Jastrow
- Gutzwiller

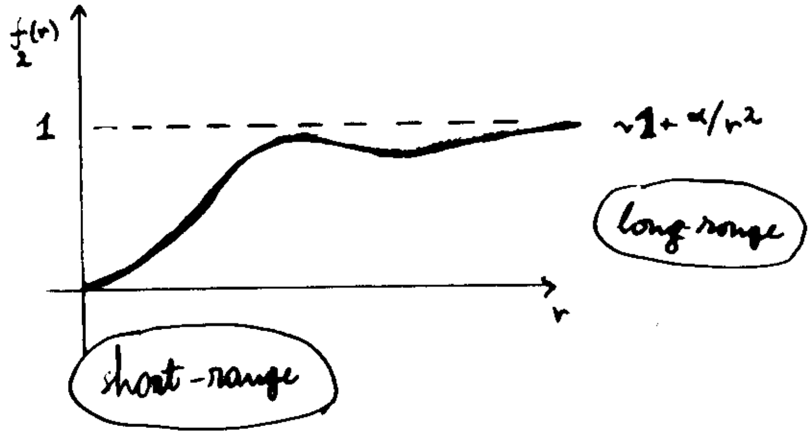

two-particle density :

spin - isospin operator $\Rightarrow \rho_{2,\alpha}$

$$\rho_2(\vec{r}_1,\vec{r}_2) = \sum_{i\neq j} \langle \delta(\vec{r}_i-\vec{r}_1)\delta(\vec{r}_j-\vec{r}_2)\rangle$$

$$\equiv \rho_1(\vec{r}_1)\,\rho_1(\vec{r}_2)\; g_2(\vec{r}_1,\vec{r}_2)$$

one - body density

$\boxed{\rho(r) = \rho \quad \text{in NM}}$

two - body distribution function

$\boxed{g_2(\vec{r}_1,\vec{r}_2) = g(r_{12}) \quad \text{in NM}}$

..... and its connection with elastic & inelastic scattering

$$\left[\begin{array}{l} S(k,\omega) = \dfrac{1}{A}\sum_I |\langle 0|\rho_k^+|I\rangle|^2\,\delta(\omega-\omega_I) \\ \rho_k = \sum_i e^{i\vec{k}\cdot\vec{r}_i} \end{array}\right.$$

$$S(k) = \int_{\omega_{el}^+}^{\infty} d\omega\; S(k,\omega)$$

$$S(k) = \frac{1}{A}\langle 0|\rho_k^+\rho_k|0\rangle - \frac{1}{A}|\langle 0|\rho_k|0\rangle|^2$$

$$\boxed{\frac{1}{A}\langle 0|\rho_k^+\rho_k|0\rangle = 1 + \frac{1}{A}\int d^3r_1\, d^3r_2\, e^{i\vec{k}\cdot\vec{r}_{12}}\,\rho_2(\vec{r}_1,\vec{r}_2)}$$

$$\Downarrow$$

$$\boxed{S(k) = 1 + \frac{1}{A}\int d^3r_1\, d^3r_2\, e^{i\vec{k}\cdot\vec{r}_{12}}\,\rho_1(r_1)\,\rho_1(r_2)\,[g(r_1,r_2)-1]}$$

Define : $\rho_2(\vec{r}_{12}) = \frac{1}{A}\int d^3R_{12}\,\rho_2(\vec{r}_1,\vec{r}_2)$

$$\rho_2(\vec{r}_{12}) = \frac{1}{(2\pi)^3}\int d^3k\; e^{-i\vec{k}\cdot\vec{r}_{12}}\,\boxed{\left\{S(k) - 1 + A|F(k)|^2\right\}}$$

$$F(k) = \frac{1}{A}\int e^{i\vec{k}\cdot\vec{r}}\,\rho_1(r)\,d^3r$$

– { pair distribution functions $g_\alpha(\vec{r}_1, \vec{r}_2)$
Static structure functions $S_\alpha(k)$ — { N-N force, Coulomb SR

– { momentum distribution $n(k)$
one-body density matrix $\rho(r_1, r_1')$ — { occupation $n(k)$

– two particle mom. dst. $n(\vec{k}_1, \vec{k}_2)$

– Dynamical structure functions $S_\alpha(k,\omega)$

$$\int d\omega \, S_\alpha(k,\omega) = S_\alpha(k)$$

{ (e,e') quenching

– Spectral functions $P_h(k,E)$, $P_p(k,E)$

$$\int_{-e_F}^{\infty} dE \; P_h(k,E) = n(k)$$

{ e,e'p background

!! – Final state Interactions = Nucleus as a target to study the propagation of N in NM

Drops of liquid ^{3}He

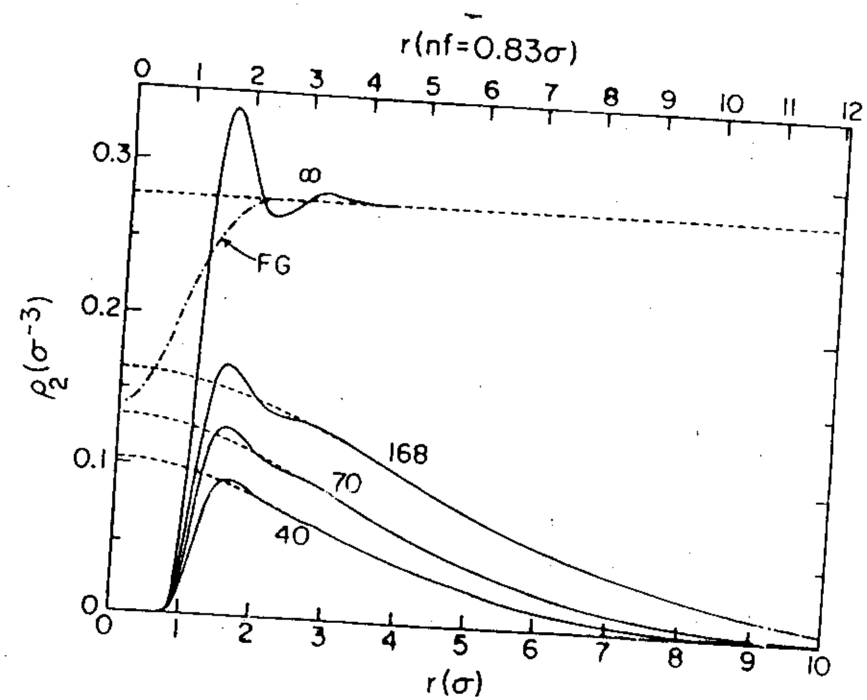

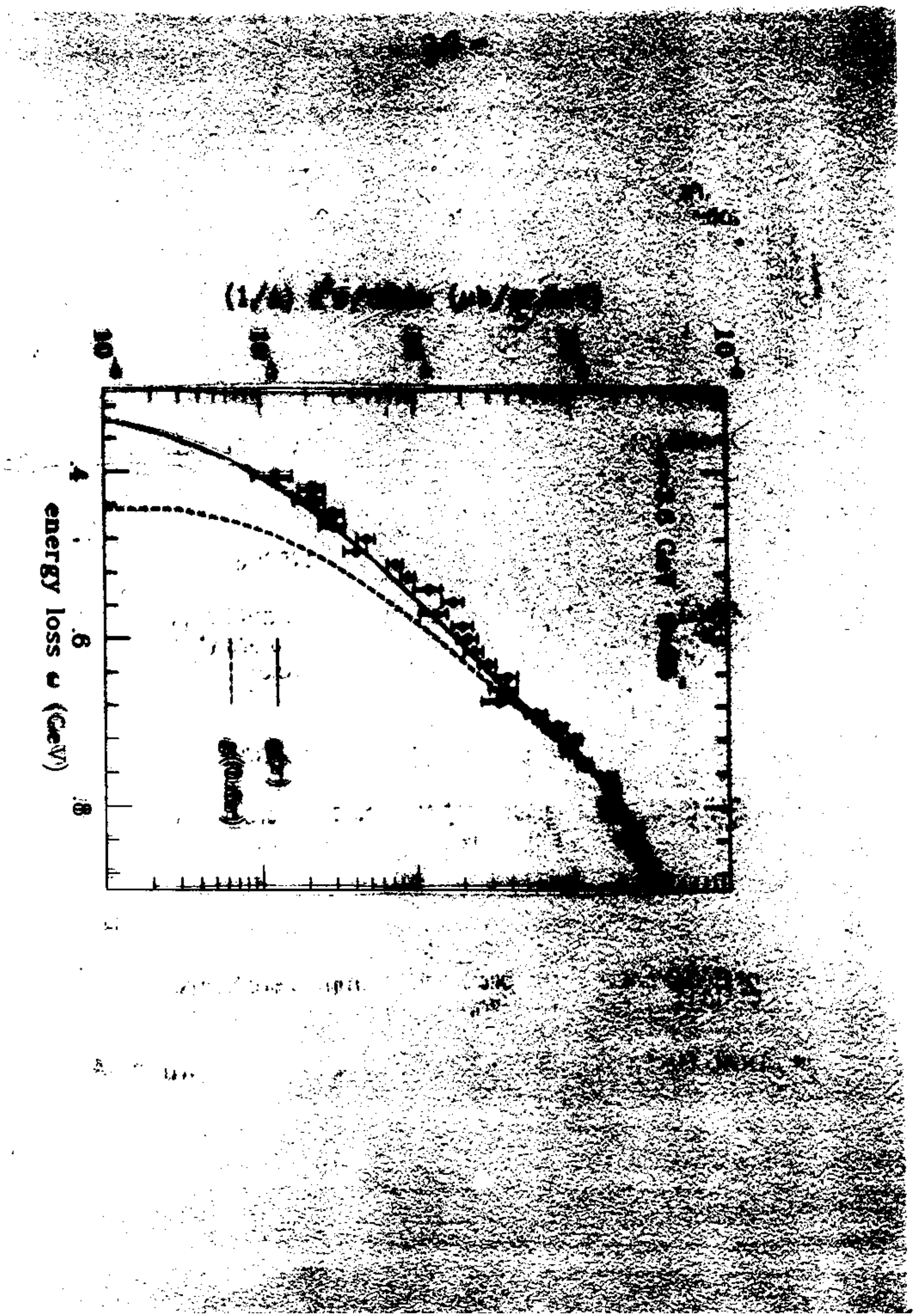

SCATTERING OF GeV ELECTRONS by NM

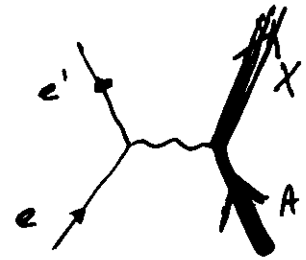

Inclusive Scattering at angle θ on

$$\boxed{{}^{4}He,\ {}^{12}C,\ {}^{27}Al,\ {}^{56}Fe,\ \text{and}\ {}^{197}Au}$$

Define

$$\Sigma_A(\vec{q},\omega) = \frac{\sigma_A(q,\omega)\left(\sigma_{ep}(q) + \sigma_{en}(q)\right)}{2\left(Z\sigma_{ep}(q) + N\sigma_{en}(q)\right)}$$

to remove from σ_A the have trivial dependence on A, Z, N and fit

$$\Sigma_A = \underbrace{\Sigma_{\text{nucl. matt.}}}_{\text{volume term}} + \underbrace{\Sigma_S\, A^{-1/3}}_{\text{surface term}}$$

- Quasi-free kinematics -

E_e (GeV)	θ	ω_{qf}	q_{qf}	v_{qf}	$\beta = \frac{1}{\sqrt{1-v^2}}$
2.02	15°	0.14	2.7	0.49	1.1
2.6	16°	0.46	5.3	0.74	1.5
3.6	25°	0.95	8.3	0.87	2.0

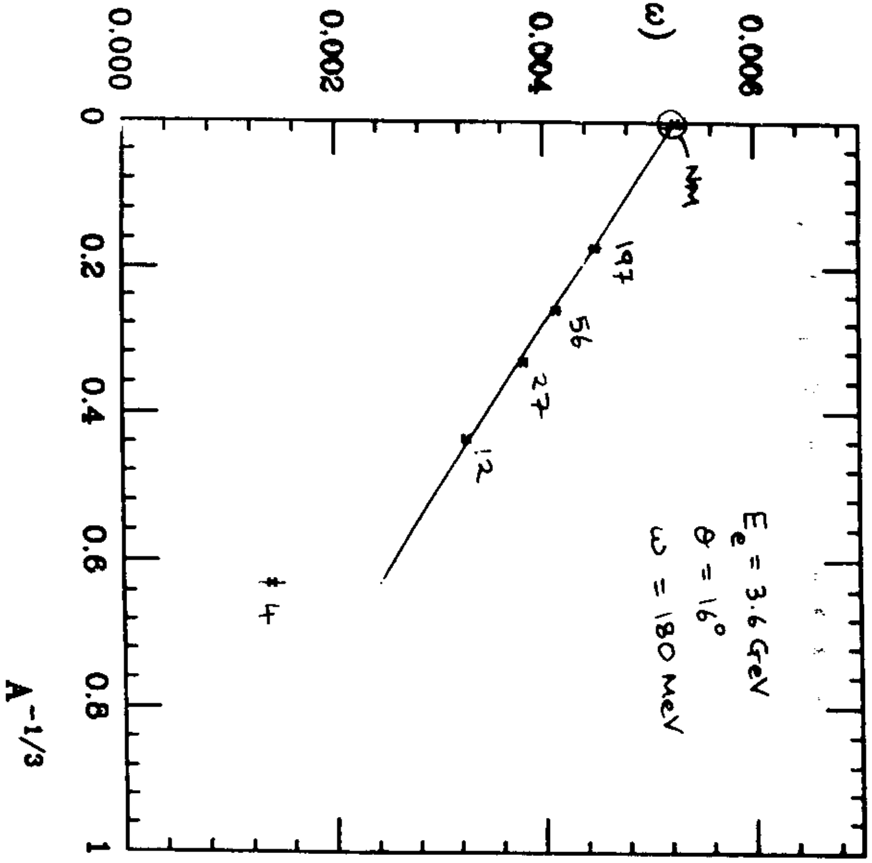

Figure 1

Extrapolated Nuclear Matter Results.

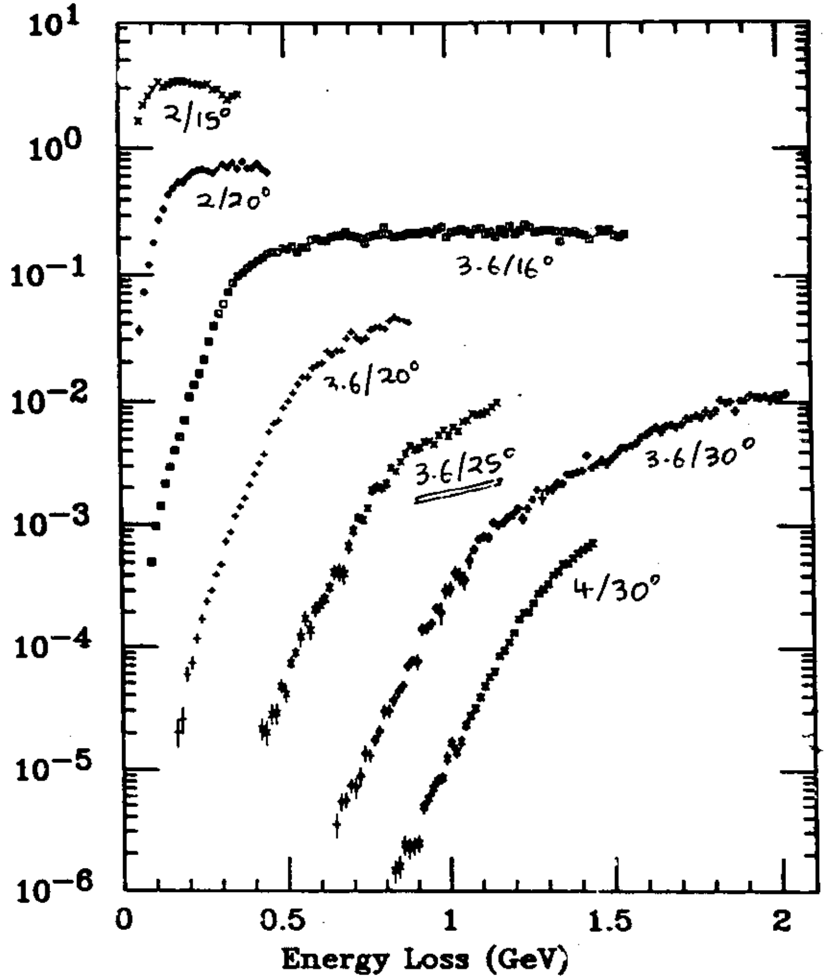

Figure 7

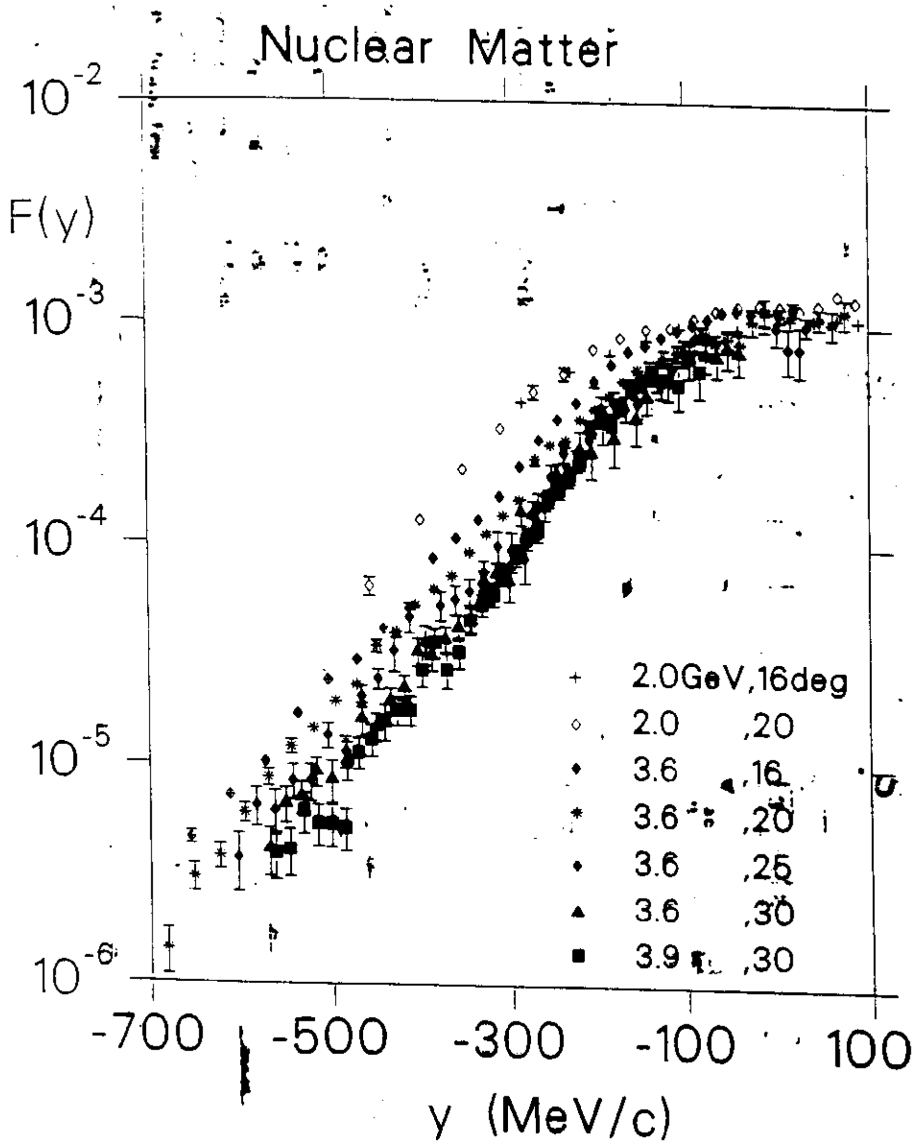

Electron - Nucleus cross section

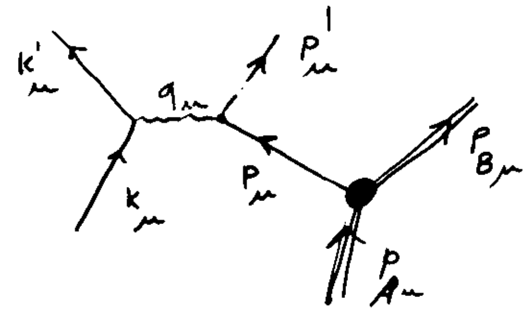

In Born approximation, the inclusive x section

$$e + A \to e' + \text{anything}$$

lepton tensor

$$\frac{d^2\sigma}{d\Omega_e\, d\varepsilon'} = \frac{\alpha^2}{q^4}\,\frac{\varepsilon'}{\varepsilon}\, L_{\mu\nu}\, W^A_{\mu\nu}(q)$$

nuclear tensor

$$\begin{cases} K_\mu = (\varepsilon, \vec{K}) \\ K'_\mu = (\varepsilon', \vec{K}') \end{cases}$$

$$q_\mu = K_\mu - K'_\mu$$

$$(K\cdot K') = \varepsilon\varepsilon' - \vec{K}\cdot\vec{K}'$$

$$\boxed{\begin{aligned} L_{\mu\nu} &= 2\left(k^\mu k'^\nu + k^\nu k'^\mu - g^{\mu\nu}(k\cdot k')\right) \\ W^A_{\mu\nu} &= \sum\!\!\!\!\!\!\int_N dp_N \langle 0|J^A_\mu|N\rangle\langle N|J^A_\nu|0\rangle \\ &\quad \times \delta(p_0 + q - p_N) \end{aligned}}$$

GAUGE Invariance + $(\mu\nu)$ symmetry imply:

$$W^A_{\mu\nu}(q) = W^A_1\left(-g_{\mu\nu} + \frac{q_\mu q_\nu}{q^2}\right) + \frac{W^A_2}{M^2_A}\left(P_{0\mu} - \frac{(P_0\cdot q)}{q^2}q_\mu\right)\left(P_{0\nu} - \frac{(P_0\cdot q)}{q^2}q_\nu\right)$$

consequently

$$\frac{d^2\sigma}{d\Omega d\varepsilon'} = \sigma_M\left[W^A_2(|\vec{q}|,\omega) + 2\tan^2\frac{\theta}{2}\, W^A_1(|\vec{q}|,\omega)\right]$$

$$\sigma_M \rightarrow \frac{\alpha^2\cos^2\theta/2}{4\varepsilon^2\sin^4\theta/2}$$

$$\frac{d^2\sigma}{d\Omega d\varepsilon'} = \sigma_M\left[\frac{q^4}{|\vec{q}|^4}R_L(|\vec{q}|,\omega) + \left(\tan^2\frac{\theta}{2} - \frac{1}{2}\frac{q^2}{|\vec{q}|^2}\right)R_T(|\vec{q}|,\omega)\right]$$

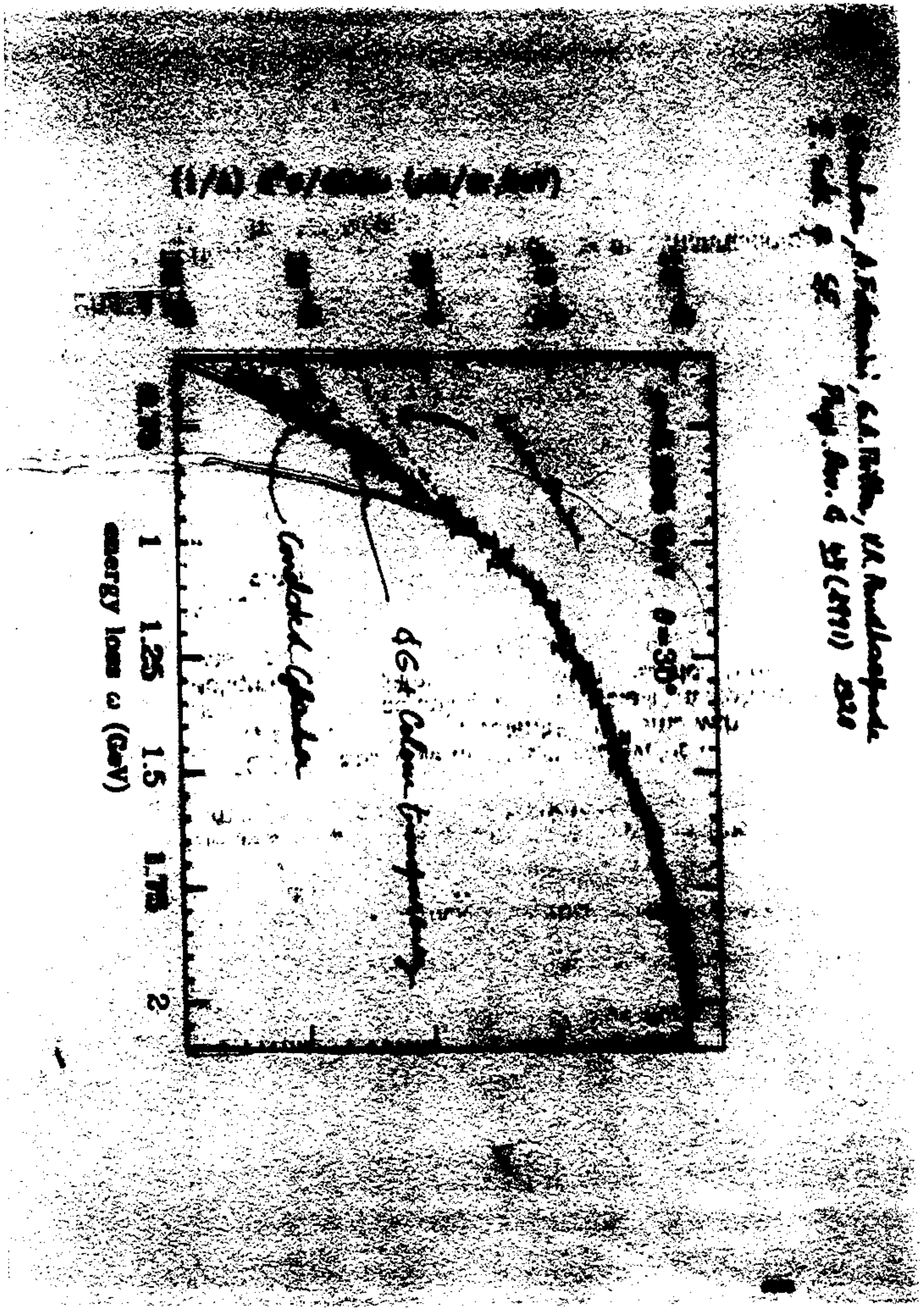

Low q regime ($q \lesssim 2k_F$)

$J = \sum J^i$ up to $\left(\frac{|\vec{q}|}{m}\right)^2$

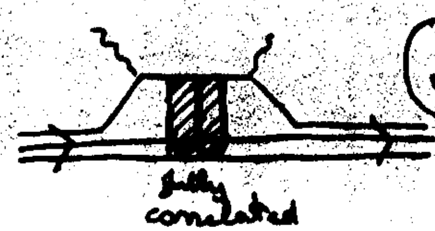

$S(q,\omega)$

High q regime

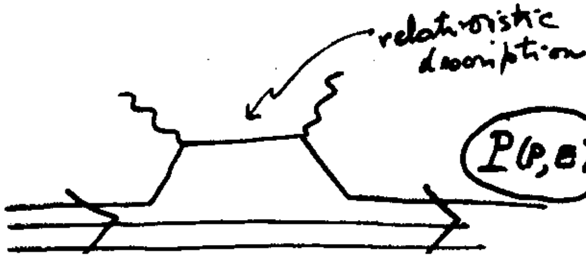

$P(p,E)$

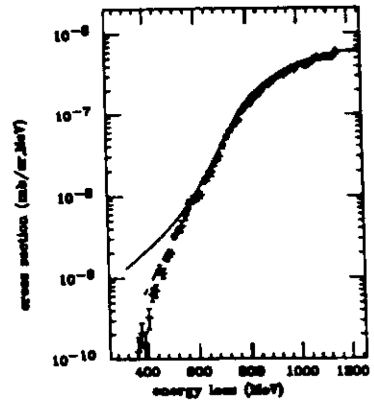

Figure 12: Inclusive cross sections for ^{56}Fe at 3.6GeV and 25°. The full LDA result (dashed line) is compared to a calculation which does not account for the reduction of final state interaction due to colour transparency (solid line).

sive scattering one does observe the *full* effect of colour transparency, as $1/q$, the distance over which (e,e') is sensitive to the interaction of the recoiling system, is comparable to or smaller than the distance within which the 'small' 3q-state evolves back to a normal nucleon. For (e,e'p), the 'standard' tool considered for the study of colour transparency, much larger q is needed to observe the full effect of colour transparency; to be specific, q has to be large enough to increase (by time dilatation) the lifetime of the small state to the time it takes to traverse the *entire nucleus*.

In figures 13 and 14 we further illustrate the quality of the results obtained. At the lower momentum transfers (figure 13) the agreement with data deteriorates somewhat at very low energy loss. The differences to experiment are very similar to the ones observed for nuclear matter. These differences are the consequence of the decreasing accuracy of Glauber theory at the lower recoil nucleon momenta. The folding function used for the description of FSI consequently is no longer as realistic as at higher nucleon momenta.

As shown by figure 14, the agreement with the data at higher momentum transfers remains very good; the quasielastic contribution (dashed line) increasingly becomes smaller relative to the large contribution of inelastic scattering on the nucleon at the larger ω.

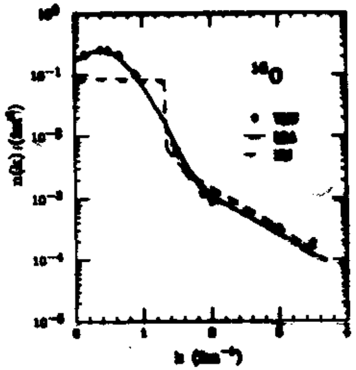

Figure 7: Momentum distribution of Oxygen: LDA (solid line), Variational Monte-Carlo calculation [illegible] (squares), nuclear matter momentum distribution, normalized to 16 nucleons (dashed).

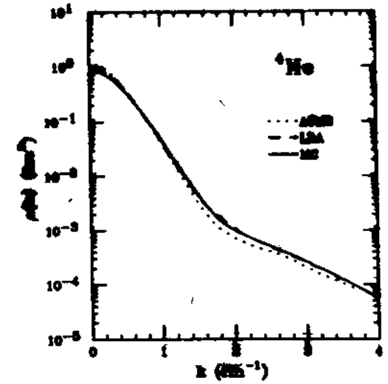

Figure 8: Momentum distribution of ^{4}He. LDA approximation (dashed), Monte Carlo calculation [illegible] (solid), ATMS calculation [4] (dotted).

21

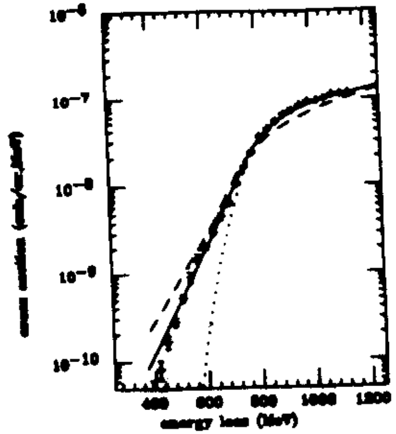

Figure 9: Inclusive cross sections for ^{12}C at 3.6GeV and 25°. LDA result (full line), calculation employing the mean-field piece of the spectral function only and no FSI (dotted), calculation using the nuclear matter spectral function and the corresponding FSI for the empirical nuclear matter density (dashed).

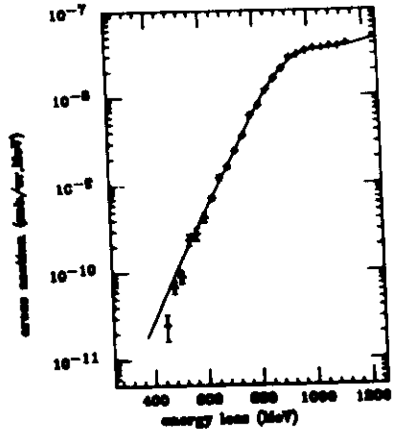

Figure 10: Inclusive cross sections for ^4He at 3.6GeV and 25°.

approximation, and the FSI treated in CGT. The calculation agrees very well with

the data, both in the region of the quasielastic peak ($\omega \simeq$ 1GeV), and in the tail at small energy loss.

The dashed curve also shown in figure 9 uses the nuclear matter spectral function for the full nuclear matter density, and the corresponding FSI. Due to the excess of high momentum components, and a final state interaction which is too strong, the cross section becomes too large at low energy loss. The dotted curve uses the mean-field part of the spectral function only, and no FSI (the long-range part of which has a small effect). This calculation also clearly disagrees with the data.

In figures 10 and 11 we show data and calculation for the same momentum transfer, but for ^4He and ^{56}Fe. Again we observe excellent agreement with the data. From this we conclude that the LDA allows to correctly treat the evolution of both spectral function and final state interaction as a function of A. Figure

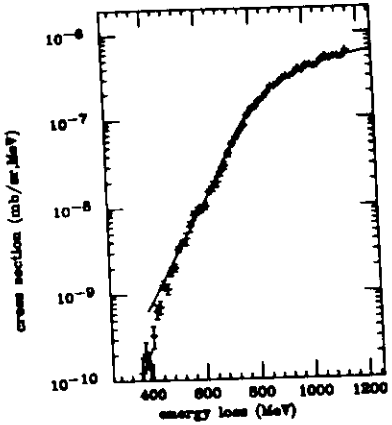

Figure 11: Inclusive cross sections for ^{56}Fe for 3.6 GeV and 25°.

12 shows for the same kinematics the iron data and calculation. While the dashed curve corresponds to the full calculation already discussed, the solid one is obtained by omitting the effect of colour transparency predicted to occur in QCD [31, 39]. Figure 12 shows that it is clearly important to include colour transparency, as it was the case for nuclear matter [11]. For ^{56}Fe the effects of colour transparency are smaller, as has to be expected given the smaller average density of the matter the nucleon recoils into.

As a matter of fact, the effect of colour transparency is still appreciable, and much larger than for (e,e'p) at the same momentum transfer. This finding, which at first sight is somewhat counter-intuitive, is explained by the fact that in *inclu-*

Benhar et al. →

Why $s\bar{s}$ systems ?

– **Diffractive electroproduction of $s\bar{s}$ mesons off nuclei**

– Color transparency:

reaction amplitude dominated by contributions from $q\bar{q}$ pairs with SMALL TRANSVERSE size $\boxed{r_s = \frac{c}{\sqrt{Q^2+m_V^2}}}$

Q increases → r_s decreases
weaker attenuation

Evidence: diffractive leptoproduction of ρ (FNAL E665)

– $c\bar{c}$ mesons, J/ψ & ψ' production (NMC) & (E691 – FNAL)

$s\bar{s}$ (s is lighter than c) needs less energy for its electroproduction
⇒ formation inside the NUCLEUS

$$e + A \longrightarrow e' + A^* + V \longrightarrow \varphi\ \varphi'$$

– incoherent –

$$\gamma^* + N \to N + V \quad \text{(elastic)}$$

restrict to $z = \frac{E_V}{\nu} = 1$

lifetime $s\bar{s}$ fluctuation of γ^* before interaction

$$\boxed{\ell_c = \frac{2\nu}{Q^2+(2m_s)^2}}$$

formation time of the vector meson

$$\boxed{\ell_f = \frac{\nu}{2m_s\,\Delta E}}$$

$\nu = 8$ GeV

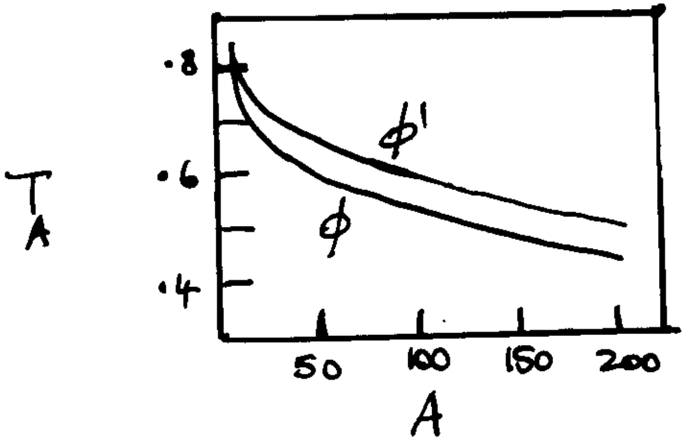

$\nu = 4$ GeV

$Q^2 = .5\left(\frac{\text{GeV}}{c}\right)^2$

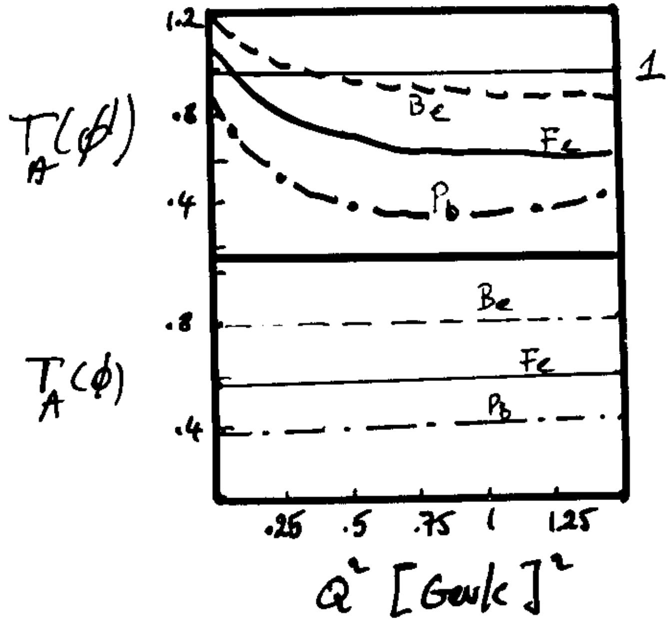

$$T'_A(V) = \frac{1}{A}\,\frac{d\sigma\,(e+A\to e'+A^*+V)}{d\sigma\,(e+N\to e'+N+V)} =$$

$$= \frac{1}{A}\,\frac{\int d^3r\,\rho_A(r)\,|\langle V|U|i\rangle|^2}{|\langle V|U|i\rangle|^2}$$

$|i\rangle = \sigma|\gamma\rangle$

interaction $s\bar{s}$ with N (2-gluon exch.)

$s\bar{s}$ component of virtual photon (Nikolaev)

Evolution of $s\bar{s}$ pair

Experiment at CEBAF